# NUMERICAL SIMULATION OF HEAT TRANSFER AND FLOW CHARACTERISTICS FOR PLATE FIN-AND-TUBE HEAT EXCHANGER WITH RING-BRIDGE SLIT FINS

***Zihao WANG[1] and Xinping OUYANG[1*]***

[*1] University of Shanghai for Science and Technology, Shanghai, China

[*] Corresponding author; E-mail: xpoy@163.com (Xinping OUYANG)

*In this paper, a new type of ring-bridge slit fins of plate fin-and-tube was proposed. It was studied by 3D numerical simulation of heat transfer and flow using FLUENT. A sample of plate fin-and-tube exchanger with ring-bridge slit fins was tested. The reliability of the simulation was demonstrated by contrasting the simulated data with the experimental data. Six different structural parameters were investigated for their effects on the flow and heat transfer performance of the plate fin-and-tube exchanger with ring-bridge fins. It was found that the fin pitch had the most significant effect on the heat transfer and flow performance of the ring-bridge slit fins. Proper reduction of the front ring-bridge slit angle of the sample was beneficial to the overall heat transfer performance. The overall heat transfer performance was weakened by both decreasing or increasing the rear ring-bridge slit angle of the sample. The optimal fin structure was obtained by the orthogonal experimental method.*

Key words*: plate fin-and-tube exchanger; ring-bridge slit fins; heat transfer enhancement; numerical simulation*

## 1. Introduction

The air conditioning and refrigeration industries both make extensive use of the fin-and-tube heat exchanger in their systems. The majority of heat exchangers is used to enable thermal transfer between air and liquid. Since the air-side thermal resistance usually makes up more than 85 % of the overall heat resistance of conventional fin-and-tube heat exchangers [1], it is necessary to develop high-efficiency fins to reduce the air-side thermal resistance, thereby improving the total heat transfer coefficient, reducing the heat transfer area of fin-and-tube heat exchangers, and reducing material consumption. The development of high efficiency fins must take into account both heat transfer performance and fluid flow pressure drop. A significant increase in fluid flow pressure drop is not necessary to achieve improvements in heat transfer performance.

Researchers have conducted numerous experimental and modeling studies in order to enhance the heat transfer efficiency of fin-and-tube heat exchangers and optimize the fluid flow pressure drops. Li [2] proposed and experimentally investigated a new kind of flat fin. The enhanced LVG (longitudinal vortex generator) fin exhibits superior heat transfer capability compared to the wavy fin, according to the entropy analysis. Kim [3] conducted an experimental research on the heat transfer and friction properties of radial slit-finned heat exchangers.

Wang [4] studied the air-side performance of a fin-and-tube heat exchanger with a flat fin structure. Wu [5] conducted experimental study on the impact of fin pitch and tube diameter on the

efficiency of air-side heat transfer in a fin-and-tube heat exchanger using a bent delta winglet vortex generator. Kong [6] found that the geometry of the slit fins can only improve the heat transfer in the mainstream zone. The continuous rectangular strip of slit fin exhibits better overall performance than the alternate upper and lower slit fin. Zhang [7] showed that the herringbone wave fin with convex strips improved heat transmission while having a slightly higher pressure drop. Li [8,9] conducted an experimental and numerical study of the heat transfer and friction characteristics of a new round-convex strip heat exchanger. The result of simulation shows that reducing the transverse tail pitch has the greatest improvement in performance.

By numerical simulation, Li [10] found that the pressure drop was biggest in the channel formed by the wavy fins. Even though it has good heat transfer, it has the worst overall performance when flow resistance is taken into account. Kumar [11] studied the effect of various parameters on the thermodynamic performance of air-cooled condensers. Numerical studies [12–16] of the thermodynamic performance of the vortex generator fins were conducted. The result shows that the arrangement of winglets reduces the wake area behind the tube. The field synergy principle is used to explain how longitudinal vortices work to enhance heat transfer.Fan [17] proposed a combination of a longitudinal vortex generator and slit parallel convex strips. Lin [18] found that the interrupted annular groove was effective in guiding and restraining the separation vortex. However, the radial and circumferential position of the annular groove has little influence on the thermal performance. Zeeshan [19] found that elliptical tubes had the best thermal-hydraulic performance among round, elliptical, and flat tubes. Zhao [20] investigated the thermodynamic performance of the air side of a rectangular elliptical fin-and-tube heat exchanger using numerical simulations. Wu [21] proposed a new type of semi-dimpled slit fin and analyzed its heat transfer and flow properties. Gholami [22] investigated the thermodynamic performance of single and triple wavy fin heat exchangers with elliptical tubes by using numerical methods. Zhi [23] considered the effects of geometric parameters and Reynold number on the thermodynamic performance of the slit fin based on a response surface methodology.

Many scholars have made great efforts to enhance air-side heat transfer and have proposed many methods to enhance heat transfer. In this paper, based on the previous research on open silt fins, a new type of open silt fin is proposed that is arranged with raised intermittent ring strips on the fins around the base tube. This kind of fin enhances heat transfer while the increase in pressure drop loss is relatively small. The raised ring-bridge structure also improves the mechanical strength of the fin. In this study, numerical simulation and test of the heat transfer and flow characteristics are carried out for this plate fin-and-tube exchanger with ring-bridge slit fins. Through orthogonal test analysis, the optimal fin structure is derived based on four structural parameters.

## 2. Experiment of plate fin-and-tube heat exchanger with ring-bridge slit fins

In this paper, a sample of a plate fin-and-tube heat exchanger with ring-bridge slit fins is first experimented with. The ring-bridge slit fin is shown in Fig. 1. The values of the convective heat transfer coefficient and the friction factor outside the tube are obtained. Subsequently, simulations are carried out on the experimental sample, and the simulation results are verified against the results of the experiments. The validated simulation method is then used to study the performance of the fin-and-tube under various working situations and structural factors.

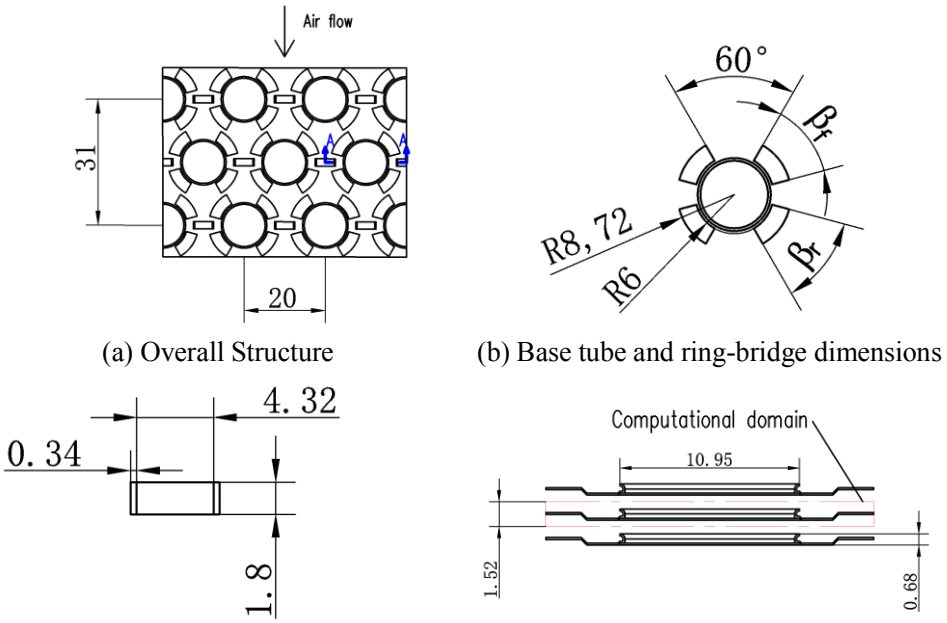


(a) Overall Structure (b) Base tube and ring-bridge dimensions

(c) Straight bridge dimension (d) Section A-A fin cross-section

**Fig.1.** Geometry of ring-bridge slit fins

The experiment was conducted on a test bench in a recirculating wind tunnel. The sample was arranged in the test section of the wind tunnel. Hot water was passed through the inside of the tube with the inlet temperature controlled at 60 ℃± 0.1 ℃, and the water flow velocity maintainedat about 1.5 m/s. The air flow velocity (face velocity) was varied from 1.5 to 4.5 m/s and the tests of seven operating points with different air flow velocities were conducted.

The basic parameters of the sample are described in Tab. 1. The geometry of the fin-and-tube is shown in Fig. 1. The heat exchanger tube is made of a C70600 copper-nickel alloy and the fin is made of C11000 red copper. There are four segments of ring-bridges around the tube and a straight bridge between two tubes.

**Tab. 1.** plate fin-and-tube diameters

| Parameter | Value |
|---|---|
| Fin pitch $F_p$ (mm) | 1.52 |
| Fin thickness $\delta$ (mm) | 0.12 |
| Base tube outer diameter $D$ (mm) | 10.35 |
| Transverse tube pitch $S_P$ (mm) | 20 |
| Longitudinal tube pitch $L_P$ (mm) | 15.5 |
| Tube length $L$ (mm) | 600 |
| Tube number M | 89 |
| Tube row $N$ | 3 |
| Slit height $h_c$ (mm) | 0.34 |
| Straight bridge height $h_s$ (mm) | 0.34 |
| Front ring-bridge angle $\beta_f$ (°) | 45 |
| Rear ring-bridge angle $\beta_r$ (°) | 45 |

## 3. Model description and numerical calculation methods

The fin-and-tube has been modeled for the experimental sample. Due to the periodic nature of the fin structure, one of the smallest periodic units of the fin-and-tube has been taken as the object of study. As shown in Fig. 1(d), the region depicted in the rectangular imaginary box is selected as the calculation domain.

As shown in Fig. 2, the actual calculation domain extends six times the longitudinal tube pitch at the inlet to maintain a constant inlet velocity and fifteen times the longitudinal tube pitch at the outlet to ensure no recirculation flow. The area width is the transverse tube pitch. As shown in Fig. 1(d), the length of the area is the transverse tube pitch. The upper boundary of the calculation domain is positioned 1 mm above the upper surface of the fin, and the lower boundary is positioned 0.4 mm below the lower surface of the fin, for a total height of 1.52 mm.

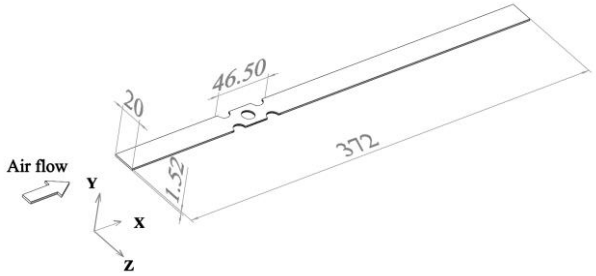


**Fig.2.** Fin-and-tube three-dimensional calculation domain

The physical parameters are taken to be constant, and the fluid is considered to be incompressible. The fluid flow is turbulent. Both the flow and heat transfer are in a steady state. The temperature of the tube wall is assumed to stay constant since the material of the tube has a high thermal conductivity, and the heat transfer coefficient inside the tube is always substantially greater than the coefficient outside the tube. The temperature of the fin surface is determined by synthetically computing the energy equation in the coupled state of air and fin.

The equations of continuity, momentum, and energy control can be described as follows:
Continuity equation:

$$\frac{\partial}{\partial x_i}(\rho u_i) = 0 \tag{1}$$

Momentum equation:

$$\frac{\partial}{\partial x_i}(\rho u_i u_k) = \frac{\partial}{\partial x_i}(\mu \frac{\partial u_k}{\partial x_i}) - \frac{\partial p}{\partial x_k} \tag{2}$$

Energy equation:

$$\frac{\partial}{\partial x_i}(\rho u_i T) = \frac{\partial}{\partial x_i}(\frac{\lambda}{c_p}\frac{\partial T}{\partial x_i}) \tag{3}$$

In this study, the effect of the boundary layer is considered including vortex and flow separation in the wake region. After considering the various scenarios that may arise during the simulation process, the Realizable k-ε model has chosen as the most suitable option.

The boundary conditions are set as follows: It is assumed that the velocity of the air entering the inlet of the calculation region is constant in the x-direction, and the air has a constant temperature $T_{in}$ and a velocity of zero in the y and z directions. The outlet condition uses the free outflow boundary condition ( $\frac{\partial u}{\partial x} = \frac{\partial v}{\partial x} = \frac{\partial w}{\partial x} = \frac{\partial T}{\partial x} = 0$ ).The left and right bounds are subject to symmetric boundary

constraints ( $\frac{\partial u}{\partial z}=\frac{\partial v}{\partial z}=0$ , $w=0$ , $\frac{\partial T}{\partial z}=0$ ). The derivative term, which is perpendicular to the boundary, is thought to be zero. The temperature of the tube wall is thought to be a constant $T_w$. The top and lower bounds are subject to periodic boundary conditions ( $\frac{\partial u}{\partial y}=\frac{\partial w}{\partial y}=0$ , $v=0$ , $\frac{\partial T}{\partial y}=0$ ). The solid surface of the model is automatically set to a no-slip boundary condition.

## 4. Parameter definition and independence verification

### 4.1. Parameter definition

The values of h, j factor, and f factor are determined by the following equations. The fluid properties are determined by the qualitative temperature.

$$h=\frac{\phi}{A_{total}\Delta T} \tag{4}$$

where $A_{total}$ is the total heat exchange area, $\Delta T$ is the log-average temperature difference, and $\Phi$ is the amount of exchanged heat.

$$A_{total}=A_{tube}+A_{fin}\eta \tag{5}$$

where $A_{tube}$ is the tube area, $A_{fin}$ is the fin area, and $\eta$ is the fin efficiency.

$$\Delta T=\frac{T_{in}-T_{out}}{\ln\frac{T_{in}-T_w}{T_{out}-T_w}} \tag{6}$$

where $T_{in}$ is the air inlet temperature, $T_{out}$ is the air outlet temperature, and $T_w$ is the outer surface temperature of the base tube.

$$j=\frac{Nu}{\mathrm{Re}\,\mathrm{Pr}^{1/3}} \tag{7}$$

$$f=\frac{A_c}{A_0}\times\frac{2\Delta p}{\rho u_{\max}^2} \tag{8}$$

where $A_c$ is the minimum flow cross-section area, $A_0$ is the total surface area, $\Delta p$ is pressure drop of air.

### 4.2. Grid independence verification

In order to perform the grid-independence verification, seven different grid cells ranging from 0.75M to 4.2M are investigated under the same conditions. The result calculated for different grid cells is shown in Fig. 3. The Nu number error calculated for the 2M and 4.2M grids is about 2 % at maximum. Therefore, considering both computational speed and accuracy, the solution of the 2M grid system can be considered as a grid-independent solution and adopted in the subsequent simulations. The error of Nu number calculated by 2M grid and 4M grid is 1.04 %. The grid diagram of the fin surface is given in Fig. 4.

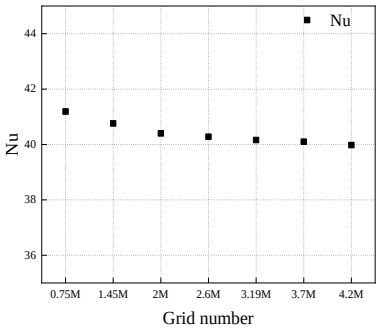


**Fig.3.** Grid-independence verification

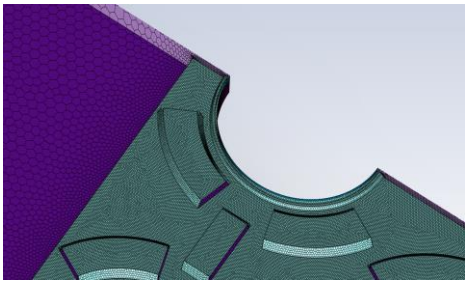

**Fig.4.** Schematic of fin surface grid

### 4.3. Validation of calculation results

To validate the computational model, the numerical simulation result of the ring-bridge plate fin-and-tube heat exchanger is compared with the experimental result.

Based on the experimentally measured fluid flow volume and inlet and outlet temperature data, the heat exchange rate and the total heat transfer coefficient can be calculated. The classical Dittus-Boelter formula is used to calculate the convective heat transfer coefficient of the water in the tube. It is possible to separate the convective heat transfer coefficient of the air outside the tube from the total heat transfer coefficient. The friction factor can be estimated using the pressure drop that isobtained experimentally.Two different turbulent models are applied in the simulation. It is shown that the heat transfer coefficient and friction factor predicted by the numerical model are compared with the outcomes of the experiments in Fig. 5.

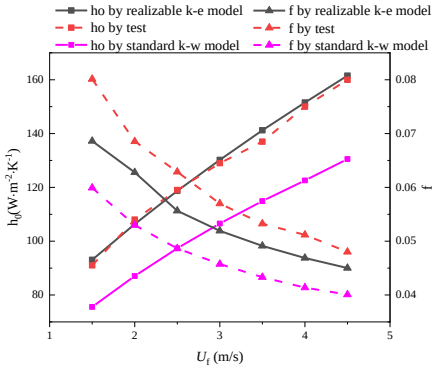


**Fig.5.** Comparison of simulated and experimental heat transfer coefficient and friction coefficient

Two different computational models are used in the simulations. For the k-ε model, the maximum error of the heat transfer coefficient is 2.97 % and the minimum is 0.25 %. The maximum error of the friction coefficient is 6.96 % and the minimum is 0.97 %. In contrast, for the k-ω model, the maximum error of the heat transfer coefficient is 18.4 % and the minimum is 16.9 %, while the maximum error of the friction coefficient is 22.7 % and the minimum is 11 %. Therefore, the k-ε model is considered more suitable for the calculation of this case and it will be used as the calculation model for similar cases of subsequent variable operating conditions or variable structures. It can be used for subsequent research analysis of fin-and-tube structure optimization.

## 5. Calculation of various cases of fin-and-tube and analysis of results

In this section, the effects of longitudinal tube pitch, transverse tube pitch, fin pitch, ring-bridge height, and front and rear ring-bridge slit angle on heat transfer and fluid flow performance are simulated and analyzed, respectively.

### 5.1. Effect of structural parameters

#### *5.1.1 The effect of longitudinal tube pitch*

The longitudinal tube pitch of the experimental sample is 15.5 mm. The simulation results, shown in Fig. 6, take into account the variation of longitudinal tube pitch from 15 mm to 16.25 mm for the same air flow velocity ($U_f$ =1.5 m/s). With increasing longitudinal tube pitch, both the j-factor and f-factorobserve to decrease. The j-factor is reduced by about 6 % and the f-factor is reduced by about 8 %. The increase in the longitudinal tube pitch makes the disturbance in the airflow weaker and the efficiency of the fin is reduced. This is the reason for the decrease in the j-factors and f-factors. In summary, the smaller the transverse tube pitch is within a reasonable range of fin structure parameters, the better the fin heat transfer performance will be.

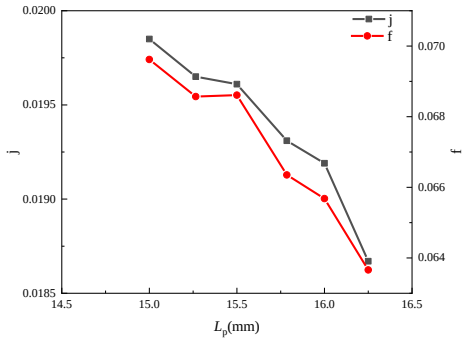


**Fig.6.** Effect of longitudinal tube pitch on j-factor, f-factor and performance index

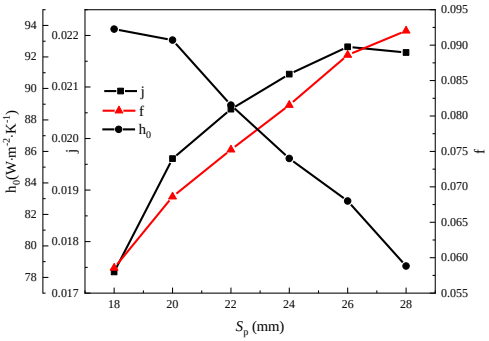


**Fig.7.** Effect of transverse tube pitch on j-factor, f-factor and heat transfer coefficient

#### *5.1.2 The effect of transverse tube pitch*

The transverse tube pitch of the experimental sample is 20 mm. The simulation simulation results, shown in Fig. 7, take into account the variation of transverse tube pitch from 18 mm to 28 mm under the same air flow velocity ($U_f$ =1.5 m/s). The results demonstrate that the heat transfer coefficient $h_o$ decreases as the transverse tube pitch Sp increases. The j-factor and f-factor increase with the increase in the tube pitch. The heat transfer coefficient is reduced by about 16 %, the j-factor is increased by about 24 %, and the f-factor is increased by about 36 %. As the transverse tube pitch increases, the flow velocity $U_{max}$ at the minimum cross-section decreases and the Re number decreases. And the efficiency of the fin is reduced. Therefore, the average heat transfer coefficient and the Nu number decrease. Since the decrease in Re number is greater than the decrease in Nu number, the j-factor exhibits an increase with increasing transverse tube pitch. Previous research theory shows that for airflow passing through the same channel, the f-factor always increases as the Re number decreases. With an increase of transverse tube pitch, the increase in circulation area makes the airflow disturbance decrease and results in a reduction in airflow resistance. However,as the Re number decreases further, the combined effect makes the f-factor increase.

### 5.1.3 *The effect of the ring-bridge slit height*

The height of the ring-bridge slit in the experimental sample is 0.34 mm. The ring-bridge slit height for simulation varies from 0.24 mm to 0.54 mm in Fig. 8. As can be observed, as the height of the ring-bridge increases, so does the j-factor and the f-factor. The ring-bridge fin enhances heat transfer in two ways: 1. Enhance the airflow disruption flow. 2. Guide the flow of gas and increase the flow of air around the tube. Both can be enhanced as the height of the ring-bridge increases. In the studied range of ring-bridge heights, the equal pump power performance evaluation index $\zeta_p$ is higher than 1 in the case of heights larger than 0.34 mm. This means that compared to flat fins, the heat exchange of a fin can only be meaningfully enhanced at fin heights greater than 0.34 mm for the same pumping power. In addition, when the height of the ring-bridge reaches 0.49 mm, the j-factor starts to decrease, and $\zeta_p$ tends to level off when the height of the ring-bridge continues to increase. Therefore, it is not necessary to continue to increase the height of the ring-bridge. It can be considered that the fin-and-tube has the best comprehensive thermodynamic performance when the height of the ring-bridge slit is 0.49 mm.

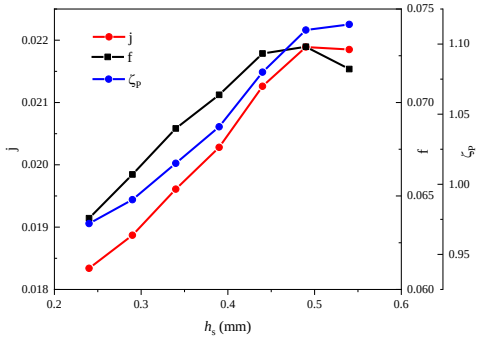


**Fig.8.** Effect of ring-bridge slit height on j-factor, f-factor and performance index

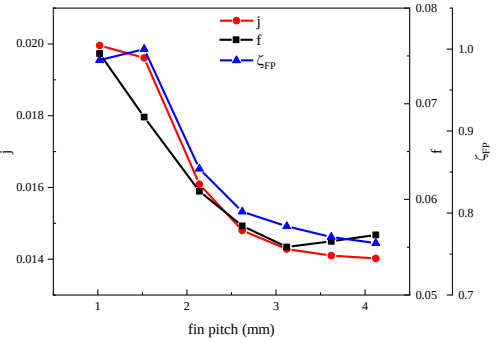


**Fig.9.** Effect of fin pitch on j-factor and f-factor

### 5.1.4 *The effect of fin pitch*

In the study of the effect of ring-bridge slit fin pitch on heat transfer performance, the fin pitch is varied from 1.02 mm to 4.12 mm. The relationship between fin pitch with j-factor, f-factor, and performance index is represented in Fig. 9. The performance evaluation index of heat transfer performance is defined as:

$$\zeta_{FP} = \frac{j_c / f_c^{1/3}}{j_{fp} / f_{fp}^{1/3}} \tag{9}$$

where $j_{fP}$ and $f_{fP}$ represent the j-factor and f-factor at a fin pitch of 1.52 mm of the sample.

The j-factor is found to decrease with an increase of fin pitch, whereas the f-factor exhibits a tendency to decrease and subsequently increase with the increase of fin pitch. Among the studied fin pitch range, the comprehensive performance evaluation indexes of other pitches are less than 1 compared to the performance index of the 1.52 mm pitch. It means that 1.52 mm has the best overall performance in the studied fin pitch range. When the fin pitch is sufficiently large, its influence on the j-factor and f-factor is negligible, according to the study [24]. Also, there should be an optimum value of fin pitch. It is shown that the result is the same as the conclusion of the study [24] in Fig. 9.

### *5.1.5 The effect of front and rear ring-bridge slit angle*

The slit angles of the front and rear ring-bridges are shown in Fig. 1(b), and those of experimental samples are 45 °. Simulations are performed by changing the slit angle of the front and rear ring-bridge, from 0 ° to 80 °, as a way to study its effect on the j-factor and f-factor. The result of the calculation is shown in Fig. 10 and Fig. 11, where $\zeta_{f0}$ and $\zeta_{r0}$ denote the comprehensive performance evaluation indexes of the variable slit angle of the front and rear ring-bridge, respectively.

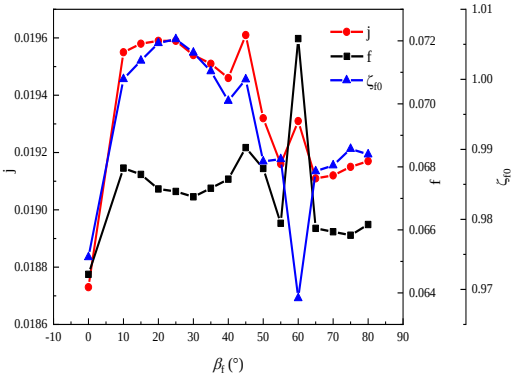


**Fig.10.** Effect of front ring-bridge angle on j-factor, f-factor and performance index

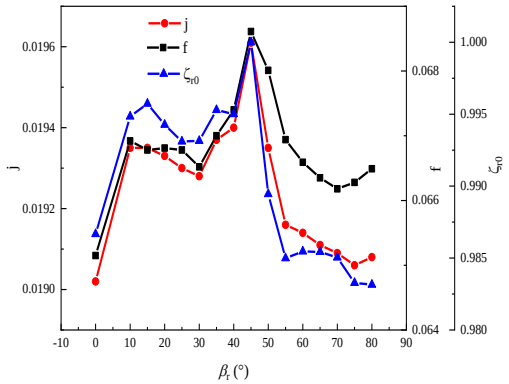


**Fig.11.**Effect of rear ring-bridge angle on j-factor, f-factor and performance index

It can be seen that both the front and rear ring-bridge slits are able to enhance heat transfer. The j-factor and f-factor show large differences with the angle changes. The ring-bridge slit can be roughly divided into two parts to enhance heat transfer: one part perpendicular to the direction of incoming flow and the other part parallel to the direction of incoming flow. The first part mainly serves to enhance the gas disturbance. The latter part is mainly to guide the gas flow, which can guide the gas flow to the wake area behind the tube to enhance the heat exchange in the wake area. Therefore, the front and rear ring-bridge slit angles contribute positively to improving the heat transfer.

In terms of performance evaluation indexes, compared to the ring-bridge slit fins of the experimental sample, the comprehensive evaluation index is higher at an angle of 15 ° to 35 ° of the front ring-bridge, reaching its highest at 25 °. It indicates that the comprehensive performance of the experimental sample should be better if the front ring-bridge angle is reduced from 45 ° to 25 °. However, the performance evaluation index is less than 1 when the rear ring-bridge angle is lower or higher than 45 ° in the sample, which indicates that the reduction or increase of the rear ring-bridge angle is not conducive to the improvement of comprehensive performance. That indicates that the disturbance effect of the rear ring-bridge slit on the rear domain of the circular tube is more effective compared to the front ring-bridge. In terms of comprehensive performance, the best angle of slit can be obtained with the front ring-bridge with an angle of 25 ° and the rear ring-bridge with an angle of 45 °.

## 5.2. Orthogonal analysis

The orthogonal analysis is a statistical analysis of the experimental results using the analysis of variance method to infer the optimal combination of multiple factors through a reasonable combination of the simulated data through an orthogonal table. Based on the numerical simulation results in sections 5.1.3 to 5.1.5, the effects of fin height, fin pitch, and front and rear ring-bridge slit

angle on heat transfer coefficient, pressure drop, and performance factor are analyzed using the orthogonal method, and the optimal combination is obtained.

The trend of the effect of fin height, fin pitch, and front and rear ring-bridge slit angle on the performance factor is obtained. Extreme difference analysis reveals that the order of the affecting factors is fin pitch > fin height > rear ring-bridge slit angle > front ring-bridge slit angle. The highest performance coefficient is obtained for the fin when the fin pitch is 1.52 mm, the ring-bridge height is 0.54 mm, the front ring-bridge slit angle is 30 °, and the rear ring-bridge slit angle is 40 °. An optimized structure is obtained by an orthogonal test with a fin pitch of 1.52 mm, a ring-bridge height of 0.54 mm, a front ring-bridge slit angle of 30 ° and a rear ring-bridge slit angle of 40 °. The numerical model of the optimized structure is built using Fluent for computational analysis. Compared to the fins with a fin pitch of 1.52 mm, a ring-bridge height of 0.34 mm, and front and rear ring-bridge slit angles of 45 °, the optimized fins improved the j-factor by 12.2 %, the f-factor by 3.1 %, the performance factor by 8.9 %, and the equal pump power performance evaluation index $\zeta_p$ by 1.111.

## 6. Conclusion

In this paper, FLUENT was used to perform a numerical simulation study of a ring-bridge slit fin, on which four ring-bridge slits are arranged around each heat exchanger tube. The accuracy of the numerical simulation results was verified by comparing them to the experimental data, and the following conclusions were drawn as:

(1) The effects of six fin-and-tube structural parameters ($L_p$,$S_p$ ,$F_p$ ,$h_s$ ,$\theta_f$ ,$\theta_r$) on the fin heat transfer and flow properties were investigated. It was discovered that the j-factor and f-factor had positive correlations with $S_p$, $h_s$ and negative correlations with $L_p$, $F_p$. Although the j-factor increases with the increase of $S_p$, the heat transfer coefficient of the fin surface reduces with the increase of $S_p$. It means that the heat transfer coefficient of the fin decreases as the $S_p$ increases. For the front and rear ring-bridge slit angles, the proper reduction of the front ring-bridge angle from 45 $^o$ of the sample to 25 $^o$ is beneficial to the overall heat transfer performance. Reducing or increasing the rear ring-bridge angle of the sample by 45 $^o$ does not improve the heat transfer performance as a whole.

(2) Within a certain range of structural parameters, the optimal fin structure was derived by orthogonal test analysis. The optimized structure improves the j-factor by 12.2 %, the f-factor by 3.1 %, and the performance factor by 8.9 %, and the equal pump power performance evaluation index $\zeta_p$ is 1.11. The overall performance is clearly better.

## Nomenclature

| | | | |
|---|---|---|---|
| $A_{fin}$ | Fin area($m^2$) | $j$ | Colburn factor |
| $A_{tube}$ | Heat exchanger tube area($m^2$) | $L$ | Tube length(mm) |
| $A_{total}$ | Total surface area($m^2$) | $L_p$ | Longitudinal tube pitch(mm) |
| $A_c$ | Minimum flow area($m^2$) | $M$ | Tube number |
| $A_0$ | Equivalent total surface area($m^2$) | $Nu$ | Nusselt number=hD/λ |
| $c_p$ | Specific heat(Jkg-1K-1) | $p$ | Pressure (Pa) |
| $D$ | Tube outside diameter(mm) | $Pr$ | Prandtl number |
| $f$ | Friction factor | $Re$ | Reynolds number=ρ$u_{max}$D/μ |
| $F_p$ | Fin pitch(mm) | $S_p$ | Transverse tube pitch(mm) |
| $h_o$ | Heat transfer coefficient outside | $T$ | Temperature(K) |

| | | | |
|---|---|---|---|
| | tube(Wm-2K-1) | | |
| $h_c$ | Height of Ring-Bridge fin(mm) | $U_f$ | Air flow velocity(m/s) |
| $h_s$ | Straight bridge height(mm) | | |

**Greek symbols**

| | | | |
|---|---|---|---|
| $\Delta P$ | Pressure drops (Pa) | $\eta$ | Fin efficiency |
| $\Delta T$ | Log mean temperature difference(K) | $\Phi$ | Heat transfer rate(W) |
| $\rho$ | Density(kg/m$^3$) | $\delta$ | Thickness of fin(mm) |
| $\mu$ | Viscosity(kgm-1s-1) | $\beta_f$ | Front ring-bridge open slit angle (°) |
| $\lambda$ | Thermal conductivity(Wm-1K-1) | $\beta_r$ | Rear ring-bridge open slit angle (°) |
| $\psi$ | Orthogonal method performance factor | $\zeta$ | Performance evaluation index |

**References**


[1] Bhuiyan, A. A. & Islam, A. K. M. S. Thermal and hydraulic performance of finned-tube heat exchangers under different flow ranges: A review on modeling and experiment. International Journal of Heat and Mass Transfer 101, 38–59 (2016).

[2] Li, M. J. et al. Experimental and numerical study and comparison of performance for wavy fin and a plain fin with radiantly arranged winglets around each tube in fin-and-tube heat exchangers. Applied Thermal Engineering 133, 298–307 (2018).

[3] Kim, N.-H. An Experimental Investigation on the Air-Side Performance of Fin-and-Tube Heat Exchangers Having Radial Slit Fins. Int. J. Air-Cond. Ref. 23, 1550021 (2015).

[4] Wang, C.-C. & Chi, K.-Y. Heat transfer and friction characteristics of plain fin-and-tube heat exchangers, part I: new experimental data. Int. J. Heat Mass Transfer 11 (2000).

[5] Wu, X. et al. Experimental study on the effects of fin pitches and tube diameters on the heat transfer and fluid flow characteristics of a fin punched with curved delta-winglet vortex generators. Applied Thermal Engineering 119, 560–572 (2017).

[6] Kong, Y. Q. Effects of continuous and alternant rectangular slots on thermo-flow performances of plain finned tube bundles in in-line and staggered configurations. International Journal of Heat and Mass Transfer 11 (2016).

[7] Zhang, K. Experimental and numerical study and comparison of performance for herringbone wavy fin and enhanced fin with convex-strips in fin-and-tube heat exchanger. International Journal of Heat and Mass Transfer 13 (2021).

[8] Li, X.-Y. et al. Experimental study on heat transfer and pressure drop characteristics of fin-and-tube surface with four convex-strips around each tube. International Journal of Heat and Mass Transfer 116, 1085–1095 (2018).

[9] Li, X.-Y. et al. Numerical study on the heat transfer and pressure drop characteristics of fin-and-tube surface with four round-convex strips around each tube. International Journal of Heat and Mass Transfer 158, 120034 (2020).

[10] Li, L. et al. Numerical simulation on flow and heat transfer of fin structure in air-cooled heat exchanger. Applied Thermal Engineering 10 (2013).

[11] Kumar, A. et al. 3D CFD simulations of air cooled condenser-III: Thermal–hydraulic characteristics and design optimization under forced convection conditions. International Journal of Heat and Mass Transfer 93, 1227–1247 (2016).

[12] Sarangi, S. K. & Mishra, D. P. Effect of winglet location on heat transfer of a fin-and-tube heat exchanger. Applied Thermal Engineering 116, 528–540 (2017).

[13] Xie, J. & Lee, H. M. Flow and heat transfer performances of directly printed curved-rectangular vortex generators in a compact fin-tube heat exchanger. Applied Thermal Engineering 180, 115830 (2020).

[14] Wu, J. M. & Tao, W. Q. Investigation on laminar convection heat transfer in fin-and-tube heat exchanger in aligned arrangement with longitudinal vortex generator from the viewpoint of field synergy principle. Applied Thermal Engineering 27, 2609–2617 (2007).

[15] Li, M. J. et al. Heat transfer and pressure performance of a plain fin with radiantly arranged winglets around each tube in fin-and-tube heat transfer surface. International Journal of Heat and Mass Transfer 70, 734–744 (2014).

[16] Wang, W. et al. Numerical investigation of a finned-tube heat exchanger with novel longitudinal vortex generators. Applied Thermal Engineering 86, 27–34 (2015).

[17] Fan, J.-F. et al. Application of Combined Enhanced Techniques for Design of Highly Efficient Air Heat Transfer Surface. Heat Transfer Engineering 33, 52–62 (2012).

[18] Lin, Z.-M. et al. Numerical study on heat transfer enhancement of circular tube bank fin heat exchanger with interrupted annular groove fin. Applied Thermal Engineering 73, 1465–1476 (2014).

[19] Zeeshan, M. et al. Numerical study to predict optimal configuration of fin and tube compact heat exchanger with various tube shapes and spatial arrangements. Energy Conversion and Management 148, 737–752 (2017).

[20] Zhao, L. et al. Numerical study on airside thermal-hydraulic performance of rectangular finned elliptical tube heat exchanger with large row number in turbulent flow regime. International Journal of Heat and Mass Transfer 114, 1314–1330 (2017).

[21] Wu, X. et al. Performance evaluation and optimization of semi-dimpled slit fin. Heat Mass Transfer 50, 1251–1259 (2014).

[22] Gholami, A. et al. Thermal–hydraulic performance of fin-and-oval tube compact heat exchangers with innovative design of corrugated fin patterns. International Journal of Heat and Mass Transfer 106, 573–592 (2017).

[23] Zhi, C. et al. Prediction and analysis of thermal-hydraulic performance with slit fins in small diameter (3 mm to 4 mm) heat exchangers. International Communications in Heat and Mass Transfer 129, 105684 (2021).

[24] He, Y. L. et al. Three-dimensional numerical study of heat transfer characteristics of plain plate fin-and-tube heat exchangers from view point of field synergy principle. International Journal of Heat and Fluid Flow 26, 459–473 (2005).

Submitted: 23.01.2023
Revised: 26.03.2023
Acepted: 28.03.2023